

DOI: 10.1002/cphc.201402236

On the Tuning of High-Resolution NMR Probes

Maria Theresia Pöschko,^[a] Judith Schlagnitweit,^[a, c] Gaspard Huber,^[b] Martin Nausner,^[a]
Michaela Horničáková,^[a, d] Hervé Desvaux,^{*,[b]} and Norbert Müller^{*,[a]}*Dedicated to Professor Heinz Falk on the occasion of his 75th birthday*

Three optimum conditions for the tuning of NMR probes are compared: the conventional tuning optimum, which is based on radio-frequency pulse efficiency, the spin noise tuning optimum based on the line shape of the spin noise signal, and the newly introduced frequency shift tuning optimum, which minimizes the frequency pushing effect on strong signals. The latter results if the radiation damping feedback field is not in perfect quadrature to the precessing magnetization. According

to the conventional RLC (resistor–inductor–capacitor) resonant circuit model, the optima should be identical, but significant deviations are found experimentally at low temperatures, in particular on cryogenically cooled probes. The existence of different optima with respect to frequency pushing and spin noise line shape has important consequences on the nonlinearity of spin dynamics at high polarization levels and the implementation of experiments on cold probes.

1. Introduction

The tuning of an NMR probe is an important routine procedure, often automated and thus invisible to users of state-of-the-art NMR systems. An optimally tuned probe should deliver a maximum signal-to-noise ratio (SNR) for the observed spins, while at the same time the radio-frequency (rf) power applied for excitation is used with optimum efficiency, that is, achieving a maximum nutation angle per energy unit.^[1,2] Moreover, apart from the direct influence of tuning on the signal-to-noise ratios of NMR signals from small magnetization, there are also remarkable effects, like radiation damping and frequency push-

ing on the NMR response of large magnetization.^[3,4] These effects are due to the precessing magnetization inducing an electric current inside the detection coil, which in turn creates a magnetic feedback field. The amplitude and the phase of this induced feedback field depend on the difference between the electronic circuit resonance frequency ω_{LC} and the nuclear spin Larmor frequency ω_0 . At perfect tuning conditions, $\omega_{LC} = \omega_0$, the feedback field is in quadrature (meaning 90° out-of-phase) to the precessing magnetization and its contribution to the spin dynamics reduces to radiation damping, which for small excitation pulses results in a broadening of the resonance line.^[3] If the tuning is not perfect the feedback field also induces a change of the observed resonance frequency of the large nuclear magnetization, called frequency pushing.^[5] Further parameters to monitor when tuning an NMR probe are the spin noise line shape, previously used to attain the spin noise tuning optimum (SNTO),^[6–8] and the radiation damping rate.^[3]

In this paper we investigate the tuning and matching dependence of conventional and cold NMR probes with respect to the SNR, radiation damping effects and line shapes in pulse and spin noise spectra. Our results are compared to previous observations^[5,7–10] and are used to propose a new tuning target, the frequency shift tuning optimum (FSTO). At the FSTO the resonance frequency of high nuclear polarization is independent of the longitudinal magnetization, which is advantageous for suppressing solvent signals on cryogenically cooled probes. According to the frequently used resistor–inductor–capacitor (RLC) model of NMR detection circuits^[11] the SNTO, and the FSTO as well as the conventional tuning optimum (CTO) should coincide. Their discrepancy has direct implications on the implementation of NMR pulse sequences in particular on cold probes and proves the inadequacy of the RLC model in many cases.

[a] M. T. Pöschko,⁺ Dr. J. Schlagnitweit,⁺ Dr. M. Nausner, Dr. M. Horničáková, Prof. N. Müller
Institute of Organic Chemistry, Johannes Kepler University Linz
Altenbergerstraße 69, 4040 Linz (Austria)
Fax: (+43) 732-2468-8747
E-mail: norbert.mueller@jku.at

[b] Dr. G. Huber, Prof. H. Desvaux
CEA, IRAMIS, NIMBE
Laboratoire Structure et Dynamique par Résonance Magnétique
SIS2M UMR CEA/CNRS 3299, CEA/Saclay, 91191 Gif-sur-Yvette (France)
Fax: (+33) 16908-2199
E-mail: herve.desvaux@cea.fr

[c] Dr. J. Schlagnitweit⁺
Current address:
Centre de RMN à Tres Hauts Champs
Université de Lyon (CNRS/ENS Lyon/UCB Lyon 1) (France)

[d] Dr. M. Horničáková
Current address:
Lohmann Animal Health
27472 Cuxhaven (Germany)

[⁺] These two authors contributed equally

 Supporting Information for this article is available on the WWW under <http://dx.doi.org/10.1002/cphc.201402236>.

 © 2014 The Authors. Published by Wiley-VCH Verlag GmbH & Co. KGaA. This is an open access article under the terms of the Creative Commons Attribution License, which permits use, distribution and reproduction in any medium, provided the original work is properly cited.

2. Results and Discussion

2.1. General Features of NMR Probe Tuning

The electronic circuit of a high-resolution NMR probe is usually represented by a coil of inductance L and resistance r , a tuning capacitor C_t in parallel to the coil and a matching capacitor C_m in series to the previous elements. In a good approximation, the first capacitor allows one to change the electronic resonance frequency ω_{LC} of the circuit to adjust it to the nuclear spin Larmor frequency ω_0 , while the matching capacitor provides for matching the impedance of the resonant circuit to the cable and amplifier impedances, that are usually 50 Ω . There are several ways to determine the optimal values of these two capacitances. Commercial NMR spectrometers provide an internal monitoring routine for tuning the probes' rf circuitry. Most commonly the minimization of the reflected power measured by a reflection bridge or by the use of a Balun circuit with a wobulator allows this procedure of probe tuning and matching.^[11] When this procedure is completed, the entire power delivered by the amplifier is optimally transformed into rf excitation by the coil and there is minimal power reflected to the amplifier, thus avoiding mismatch conditions. This is of particular importance when long and intense rf irradiations are used, for example, for decoupling or transferring magnetization at Hartmann-Hahn conditions.^[12] We refer to this well-known procedure as finding the conventional tuning optimum (CTO). Signal-reception is performed by a different part of the circuit, which is activated by a transmit/receive (TR-)switch or through the intrinsic properties of crossed diodes.^[11] It was shown previously by noise measurements that, even if this classical tuning is done very accurately, most of the time, it is not optimal with respect to signal reception.^[7,8,13] One can optimize for signal reception by maximizing the received electronic noise power or, largely equivalent, by optimizing a nuclear spin noise line shape to appear as a symmetrical dip in the noise baseline, as reported previously.^[6-8] This alternate tuning procedure, which was called spin noise tuning optimum SNT0^[8] can result in higher SNR for NMR signals, when the noise digitization is the limiting quantity.^[7,13]

2.2. Three Different Tuning Criteria

To compare the performance of a cryogenically cooled probe, in which the temperature of the resonant circuit is significantly below the one of the sample, under different tuning and matching conditions, we systematically monitored different parameters on a sample composed such that both high and low spin magnetizations are present. Using a 500 MHz cryo-probe, which had been used in a number of previous investigations,^[8,13-15] line shapes of spin noise signals, rf pulse lengths proportional to $1/\gamma B_1$ (with γ the gyromagnetic ratio and B_1 the rf amplitude), and frequency shifts f_s^0 caused by the frequency pushing effect^[9,10] were determined under a variety of conditions. The results are summarized in Figure 1 and in the Supporting Information.

From Figure 1 three special conditions can be defined as follows: (1) γB_1 is maximum at a given rf power delivered by the rf amplifier (CTO condition), (2) the line shape of the spin noise signal is a symmetrical dip of the noise baseline (SNT0 condition), and (3) the frequency shift of a high polarization signal is zero, which we call the frequency shift tuning optimum (FSTO condition).

It is noteworthy that, in addition to what was found in previous investigations,^[7,8] there is an infinite number of (C_t , C_m) combinations where the spin noise signal appears as a symmetrical dip line shape (see Figure 1). This degeneracy results from the fact that the SNT0 is obtained, whenever the imaginary part of the receiver circuit impedance vanishes, that is, a single physical condition for two adjusted parameters, C_t and C_m . The position, where the frequency pushing effect is minimal, lies between the CTO and the SNT0 condition, at which the signal-to-noise ratio is a maximum. Similarly to the spin noise studies,^[7] this mistuning with respect to the SNT0 condition can lead to a decrease of the SNR for low receiver gain values (the meaning of "low" depending strongly on the specific hardware used). When high gains can be used to ensure appropriate digitization of noise, no SNR loss is observed.

2.3. The Frequency Shift Tuning Optimum

As described previously in ref. [3] and ref. [4], the precessing magnetization M_+ creates the feedback field ω_1 due to the detection circuit:

$$\omega_1 = i \frac{\mu_0 \gamma \omega_0 \eta Q}{2\omega_{LC} \sqrt{1 + \Delta_{LC}^2}} e^{-i\psi} M_+ \quad (1)$$

where μ_0 is the magnetic permeability of free space, γ the gyromagnetic ratio, η the filling factor and Q the apparent quality factor of the loaded resonant circuit with the sample inside. In this equation, both Δ_{LC} and ψ depend on the mistuning between the Larmor frequency ω_0 and the electronic circuit resonance frequency ω_{LC} :

$$\Delta_{LC} = Q \frac{\omega_{LC}}{\omega_0} \left[\frac{\omega_0^2 - \omega_{LC}^2}{\omega_{LC}^2} \right] \quad (2)$$

$$\psi = \arctan \Delta_{LC} \quad (3)$$

The angle ψ thus represents the deviation of the radiation damping field from quadrature of the precessing magnetization. In the context of the here-reported experiments and more generally for all high-resolution NMR experiments, since the extent of mistuning is in the order of a few hundreds of kHz for Larmor frequencies in the order of several hundreds of MHz, one can simplify the expression of Δ_{LC} as:

$$\Delta_{LC} \approx 2Q \frac{\omega_0 - \omega_{LC}}{\omega_0} \quad (4)$$

The so-called frequency pushing effect^[5] results from the imaginary part of the feedback field induced by the rf coil not

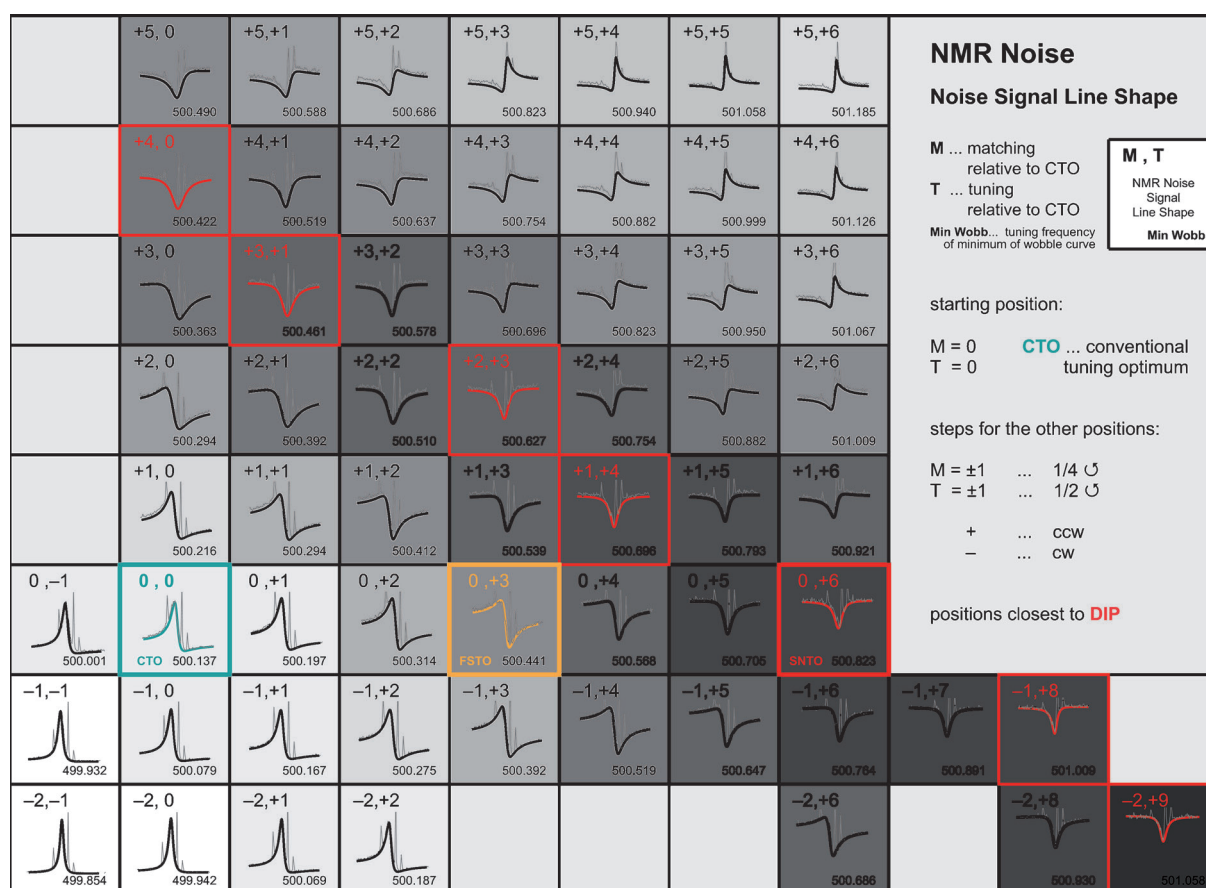


Figure 1. Map of ^1H spin noise spectra of the sample acetone:acetonitrile:chloroform (1:0.07:0.17) + 5% $[\text{D}_6]\text{DMSO}$ by volume, recorded on a 500 MHz Bruker DRX spectrometer equipped with a TXI cryo-probe for different tuning and matching positions. The bold traces are noise signals of acetone, which were deconvolved to avoid interference caused by the narrow superimposed signals of the ^{13}C satellites and of acetonitrile. Tuning/matching combinations, where spin noise signals form dips, are indicated by red frames. The FSTO (as found through small-flip angle pulse spectra, see Supporting Information) is highlighted in yellow, while a cyan-colored frame denotes the conventional tuning optimum (CTO), where γB_1 is maximum. Different shades of grey indicate the circuit's thermal noise power level at each position (darker greys correspond to higher values).

being perfectly orthogonal to the transverse magnetization [Eq. (1)].^[3] The frequency pushing f_s^0 can be described analytically by Equation (5):^[10]

$$2\pi f_s^0 = \lambda_R^0 \frac{\Delta_{\text{LC}}}{1 + \Delta_{\text{LC}}^2} \quad (5)$$

λ_R^0 is the radiation damping rate at perfect tuning ($\omega_{\text{LC}} = \omega_0$) and at thermal equilibrium between coil and spin system:

$$\lambda_R^0 = \frac{\mu_0}{2} |\gamma| \eta Q M_0 \quad (6)$$

where M_0 is the longitudinal magnetization at equilibrium with the temperatures $T_{\text{circuit}} = T_{\text{sample}}$.

The observed resonance full line width at half height for large magnetization, high Q , and small flip angle excitation pulses is $(\lambda_R + \lambda_2)/\pi$, with λ_2 being the transverse self-relaxation rate of the observed species and λ_R the effective radiation damping rate which depends on the tuning conditions:

$$\lambda_R = \lambda_R^0 \frac{1}{1 + \Delta_{\text{LC}}^2} \quad (7)$$

To assess these effects experimentally in a systematic way, we obtained small flip angle (SFA) pulse and spin noise ^1H NMR spectra under different tuning conditions on a sample of acetone using a cold probe. The results shown in Figure 2 illustrate the positions and characteristics of the three different tuning optima. In panels a and b SFA and spin noise spectra at different tuning offsets are compared. In Figure 2c the experimentally determined line widths obtained from the small flip angle spectra of Figure 2a are plotted as a function of the tuning offset. The line widths are dominated by the radiation damping term and equal to $(\pi\lambda_R)^{-1}$ under the experimental conditions of Figure 2. Comparing this plot to the one in Figure 2d shows that radiation damping is at its maximum at tuning conditions where the frequency pushing effect vanishes, as pointed out earlier by Torchia.^[10] Panels c and d of Figure 2 also provide experimental evidence that radiation damping and frequency pushing described by Equations (7) and (5), respectively, are the absorptive and dispersive components of the same effect. Figure 2 also corroborates that on a cryo-probe the difference between the SNT0 and FST0 conditions is much larger than the uncertainty of determining the respective tuning conditions.

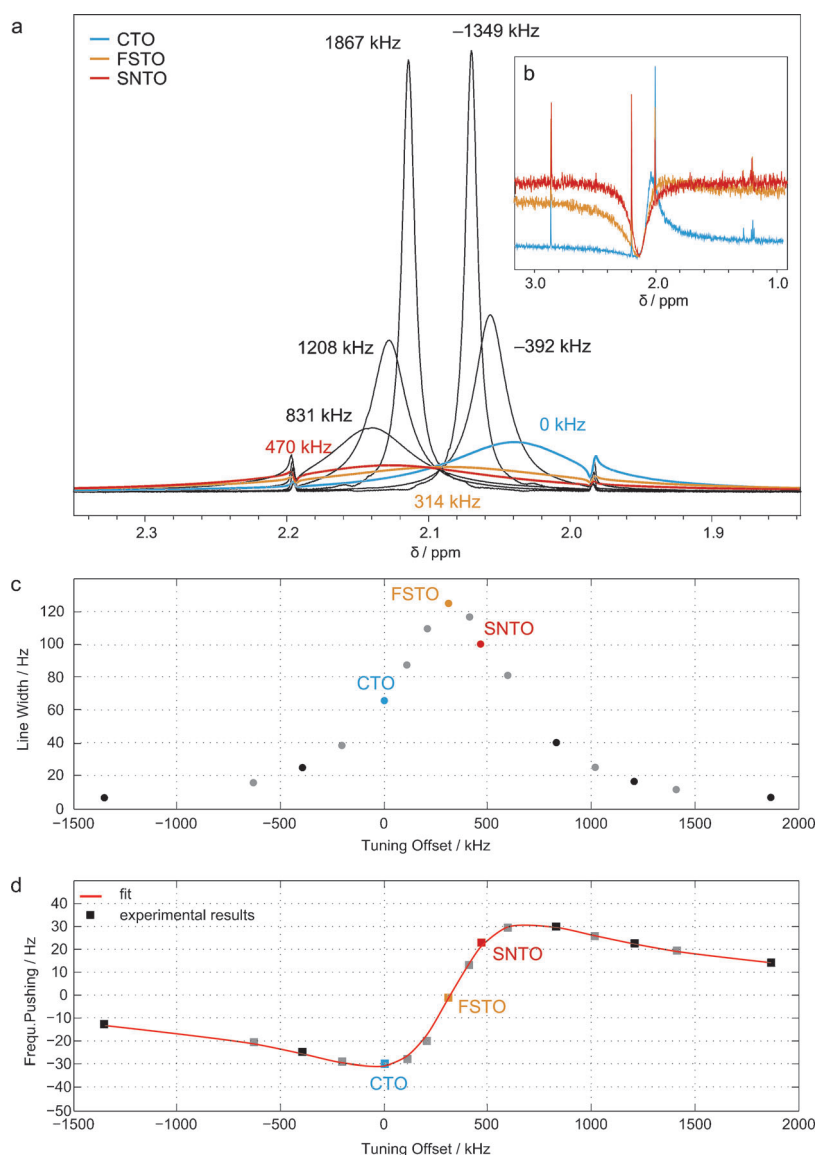


Figure 2. Variation of ^1H line shapes and resonance frequency shifts of 90% of acetone in $[\text{D}_6]\text{DMSO}$ as a function of the tuning frequency of the electronic detection circuit of a 600 MHz cryo-probe. Colors represent different tuning frequencies ranging from -1.4 MHz up to 1.9 MHz relative to the CTO condition, which is shown in cyan. The FSTO and the SNTO conditions are indicated by yellow and red, respectively. To take into account the variation of detection sensitivity due to the tuning offset, the spectra were normalized to the residual $^1\text{H}_2\text{O}$ signal ($<0.5\%$ in $[\text{D}_6]\text{DMSO}$), whose concentration was sufficiently low not to be affected by radiation damping. Panel (a) shows small flip angle spectra for various tuning positions with numerical values of the corresponding tuning offsets. The inset panel (b) displays the spin noise spectra only at the three characteristic optimum tuning conditions. The observed line widths and frequency shifts are plotted in the panels (c) and (d), respectively, as functions of the tuning offset relative to the CTO, the experimental points correspond to the spectra shown in (a). The best-fit curve to Equation (5) is drawn in red in panel (d). It is represented by a Q of 800, $\omega_{\text{FSTO}}/2\pi = 599.596$ MHz and $\lambda_{\text{R}}^0/\pi = 124$ Hz. The observed deviation of the SNTO from the FSTO frequency $(\omega_{\text{SNTO}} - \omega_{\text{FSTO}})/2\pi = -156$ kHz is caused by the feedback field. For clarity, the small flip angle spectra corresponding to the grey dots in (c) and (d) are not included in (a).

On all cryo-probes we investigated the FSTO was found between the CTO and the SNTO. Since the three tuning conditions (CTO, SNTO and FSTO) correspond to three different ω_{LC} values, we shall in the following denote them as ω_{CTO} , ω_{SNTO} and ω_{FSTO} , respectively, and similarly we shall use Δ_{CTO} , Δ_{SNTO} and Δ_{FSTO} instead of Δ_{LC} as appropriate. It is noteworthy and it may be of practical relevance that radiation damping is not at

its maximum under SNTO conditions, but coincides with the FSTO [Eqs. (5) and (7)].

In general, the frequency shift as well as the radiation damping rate scale as the longitudinal magnetization M_z , that is $f_s = f_s^0(M_z/M_0)$ and $\lambda_{\text{R}} = \lambda_{\text{R}}^0(M_z/M_0)$. Thus both f_s and λ_{R} depend on the temperature ratio between circuit and sample. This explains the extraordinary tuning behavior of cryogenically cooled probes.^[8,13] By using Equation (4) from ref.[16], the effective circuit temperature can be determined from the concentration dependence of the spin noise signal shape and offset. As a consequence of the frequency pushing effect, the peak position becomes dependent on M_z unless $\omega_{\text{FSTO}} = \omega_0$. Therefore, $\omega_{\text{FSTO}} = \omega_0$ represents a very favorable situation for solvent suppression, since the solvent peak position does not depend on its z -magnetization. It consequently facilitates the fine adjustment of the solvent suppression technique and reduces drift artifacts during long-time experiments, since the frequency pushing on the solvent resonance will not change due to varying solvent magnetization. To be more accurate, a residual longitudinal magnetization dependence of the observed resonance frequency on the order of 1 to 3 Hz remains present (assuming typical high resolution NMR conditions), since, for a nonspherical sample and large magnetization, the exact resonance frequency is affected by long-distance dipolar fields.^[4] While in principle homogeneity fluctuations may also cause variations in the Larmor frequency, these will usually be corrected by the field frequency lock, which is much less affected by the radiation field (due to low γ of the lock nucleus D). These fluctuations do not lead to appreciable spin-circuit mistuning, because they are in the Hz range, while tuning offsets having an effect on the resonance frequency and line shape are in the kHz range.

Since the frequency shift tuning optimum FSTO can be determined very precisely from a series of single small flip angle pulse experiments (Figure 2) by fitting to Equation (5),^[17] or interactively using the isosbestic behavior shown in Figure 2a we suggest to use it as an alternative tuning optimum, in cases where optimal control of the feedback field properties is sought.

2.4. Conventional NMR Probes

We conducted similar studies with conventional high resolution NMR probes (where the resonant circuit and the sample are at the same temperature), exploring tuning settings corresponding to CTO, SNT0 and FSTO conditions. The smaller quality factors Q of conventional probes reduce the magnitudes of the radiation damping rate [Eq. (6)] and of the frequency pushing effect [Eq. (5)]. Nevertheless by contrast to cold probes, other experimentally accessible degrees of freedom exist. The adaptation of the cable lengths between the TR-switch, the preamplifier and the probe has allowed us to explore the effect of changing the impedance of the transmission line on the observed signals. This feature was previously used for ensuring correct amplifier matching conditions in the SNT0 conditions,^[6,7] and was recently employed to study the influence of systematic variation of cable lengths on spin noise line shapes.^[18]

We compared spin noise and small flip angle spectra for different cable lengths between the TR-switch and the probe. We observed that the frequency shifts almost vanished at the SNT0 conditions: the differences between the FSTO and SNT0 conditions were much smaller than in the case of cryo-probes and typically within the measurement uncertainties for defining the SNT0. In the Supporting Information, spin noise spectra acquired with different cable lengths are shown. As also observed on the small-flip angle spectra,^[17] the resonance line widths vary. They clearly prove that the signal shapes can be affected by the transmission line impedance beyond the detection coil and associated capacitor. This "remote impedance effect" was further confirmed by noting a small but detectable dependence on the observed SNT0 and FSTO positions on the spectrometer receiver gain levels. These sets of experiments illustrate that tuning conditions are influenced by all reception circuit components and not by the probe circuit alone.

2.5. Reconciling FSTO and SNT0?

While it follows from the usage of a T/R-switch or crossed diodes that the CTO can deviate from the reception optimum, the observation of different values for FSTO and SNT0 appears counter-intuitive. Indeed assuming, as usual, that the detection circuit can be represented by an RLC circuit resonance, following McCoy and Ernst,^[19] the nuclear spin noise spectral density W^u is:

$$W^u(\omega) = W_c^u \frac{1 + \lambda_R^0 a(\omega)}{[1 + \lambda_R a(\omega)]^2 + [\lambda_R d(\omega) + \Delta_{\text{SNT0}}]^2} + W_a^u \quad (8)$$

where W_c^u is the spectral density of the resonant electronic circuit, W_a^u is noise spectral density of other sources such as the preamplifier, and $a(\omega)$ and $d(\omega)$ are the absorptive and dispersive NMR resonance line shapes:

$$a(\omega) = \frac{\lambda_2}{\lambda_2^2 + (\omega - \omega_0)^2} \quad (9)$$

$$d(\omega) = \frac{\omega - \omega_0}{\lambda_2^2 + (\omega - \omega_0)^2} \quad (10)$$

When perfect tuning conditions (SNT0)^[19] are fulfilled, that is:

$$\Delta_{\text{SNT0}} \simeq 0 \quad (11)$$

Equation (8) becomes:

$$W^u(\omega) = W_c^u \left[1 - \frac{\lambda_R^2 + 2\lambda_R^0\lambda_2 - \lambda_R\lambda_2}{(\lambda_R + \lambda_2)^2 + (\omega - \omega_0)^2} \right] + W_a^u \quad (12)$$

For the case $T_{\text{circuit}} = T_{\text{sample}}$ it follows that $\lambda_R = \lambda_R^0$ and therefore Equation (12) reduces to a simple Lorentzian-like function, the symmetrical dip line shape observed at the SNT0:

$$W^u(\omega) = W_c^u \left[1 - \frac{\lambda_R^0 + \lambda_R^0\lambda_2}{(\lambda_R^0 + \lambda_2)^2 + (\omega - \omega_0)^2} \right] + W_a^u \quad (13)$$

Comparing Equations (5) and (8) reveals similar dependence of the frequency pushing effect and the spin noise line shape on the tuning frequency offset. The frequency pushing consequently should also vanish at the SNT0. This comparison also illustrates that Δ_{SNT0} is the appropriate dimensionless parameter to describe the mistuning. For conventional probes used at room temperature, it is impossible to assess that SNT0 conditions are fulfilled, if the deviation is less than about $\Delta_{\text{SNT0}} = 0.05$ for a restricted time of spin-noise signal averaging (see Supporting Information). This leads to a potential small dispersive contribution on the spin noise line shape and an ensuing misinterpretation of the resonance frequencies. As a consequence, for these probes SNT0 and FSTO conditions are identical within experimental uncertainties. But for cold probes (as in Figure 2), the difference

$$\varepsilon = \Delta_{\text{SNT0}} - \Delta_{\text{FSTO}} \quad (14)$$

deviates significantly from zero, that is, a discrepancy between the two ω_0 values determined from Equation (5) and Equation (8), which define the FSTO and SNT0 conditions is observed.

This proves that the entire detection circuit cannot be reproduced by a simple RLC resonant circuit model, since it is not sufficient to describe all physical phenomena (i.e. spin noise line shapes and frequency pushing) related to NMR signal detection, as is most evident on cryogenically cooled probes. An improved model should allow the design of probes, where the differences between the three optima vanish.

The set of experiments acquired with room temperature probes described in the Supporting Information corroborates the cable length dependence reported earlier.^[18] This shows that the spin dynamics depend on the preamplifier and the TR-switch. Similarly, resonance frequencies and line widths were observed to depend on the receiver gain levels for cold probes by comparing spectra acquired at the same tuning frequency but at different receiver gain levels. Moreover a significant difference was observed when comparing the line widths [Eq. (7)] and the resonance frequencies [Eq. (5)] as functions of the tuning conditions, at constant receiver gain levels, in a procedure similar to that used to obtain Figure 2. The analysis indicates a variation of the extracted apparent Q values by 7.5% over the whole range of receiver gains. This translates into a theoretical variation of the signal-to-noise ratios of 3.5%.^[1] The practical consequences are obviously different since the receiver gain levels have an influence on the digitization noise. Associated with this Q variation, the FSTO was observed to vary to an extent of the order of $\Delta_{\text{FSTO}}=0.05$. Even if this receiver gain influence is significant and clearly detectable at the FSTO, it is not sufficient to allow reconciliation of the SNTO and FSTO conditions, since for instance in the case of the cryo-probe in Figure 2 we found a deviation $\Xi = -0.4$.

In further attempts to characterize the difference between FSTO and SNTO, the relative noise levels originating from the preamplifier and from the electronic circuit resonance (coil and sample) were varied. On a conventional probe it became possible to clearly distinguish FSTO and SNTO by decreasing the sample and coil temperatures down to -60°C (see the Supporting Information). Here, by adjusting the impedance of the transmission line, it was possible to render the three optimum conditions (CTO, SNTO and FSTO) indistinguishable. This is in contrast to a cryo-probe, where the transmission line impedance between coil and preamplifier is invariable. But by increasing the sample conductivity through the addition of salt (Table 1 and Figure S4 in the Supporting Information) we were able to reduce the difference Ξ significantly. Apparently the increased salt concentration caused a higher total noise level from the receiving coil assembly making the situation more comparable to a conventional probe. From Table 1 it is evident that, while the apparent difference of the two tuning frequencies increases with the ionic strength, the dimensionless parameter Ξ decreases. These two sets of experiments substanti-

ate the key importance of electronic components beyond the probe on the manifestation of different SNTO, FSTO and CTO conditions.

3. Conclusions

Our results from a plethora of different probes (we have run similar experiments, albeit not as systematic and thorough as the ones reported here, on at least seven different probes and spectrometers) consistently show that, there are three different "optimal" tuning and matching combinations on cold probes. Usually probes are optimized for optimum pulse performance at the CTO. The two other optima (SNTO and FSTO) are most often indistinguishable on conventional probes at room temperature, but they can be significantly different at lower temperatures and in particular for cryogenically cooled probes.

Each of the tuning optima provides different benefits depending on the requirements of the sample and the type of experiment. The conventional tuning optimum CTO allows for the shortest pulse lengths. It should be used whenever excitation efficiency is most important. At the frequency shift tuning optimum, FSTO, radiation damping is at its maximum and there is no frequency pushing effect, which means that the feedback field is in perfect quadrature to the transverse magnetization. Using the FSTO is advantageous for solvent (water) signal suppression experiments, since the solvent resonance position is not shifting as a function of total z-polarization. It thus provides conditions for more stable solvent suppression even in cases where the homogeneity fluctuates during an experiment or where the solvent concentration changes, for example, through evaporation. At the SNTO we find optimum reception conditions, that provide signal-to-noise gains for small receiver gains. It is also the most favorable condition for spin noise imaging^[14] and spectroscopy, in particular the recently introduced 2D variant.^[20]

Comparing experimental results to theoretical predictions it becomes clear that the simple RLC model for describing the NMR electronic probe circuit cannot explain these differences. The FSTO and SNTO conditions are dependent on the input impedance of the preamplifier, which varies with the receiver gain, and on the cable length between the probe and the preamplifier, as well as on the conductivity of the sample. Inclusion of additional probe components including the transmission line, the preamplifier and their temperatures will therefore be required in future theoretical models.

Experimental Section

Determination of the SNTO and the Tuning-Matching Map

The data shown in Figure 1 for the 500 MHz cryo-probe were obtained on a 2003 model Bruker TXI cryo-probe connected to a DRX console. To minimize the impact of electronic noise generated by the pulse amplifier and other spectrometer hardware the main supply of the proton pulse amplifier was turned off and the BNC-connector to the proton pre-amplifier was replaced by a $50\ \Omega$ terminator while acquiring spin noise spectra. While it is straightforward to trace the actual tuning position as the frequency offset of

Table 1. Differences between the FSTO and SNTO frequencies and corresponding mistuning parameters Ξ [Eq. (14)] as a function of the salt concentration c_{NaCl} in a $\text{H}_2\text{O} : \text{D}_2\text{O} = 1:1$ sample on a 700 MHz TCI cryo-probe (see Supporting Information).

c_{NaCl} [mmol L^{-1}]	$(\omega_{\text{SNTO}} - \omega_{\text{FSTO}}) / 2\pi$ [kHz] ^[a]	Ξ ^[a]
0	-236 ± 19	-0.42 ± 0.05
100	-235 ± 29	-0.20 ± 0.03
200	-318 ± 38	-0.20 ± 0.03
300	-335 ± 28	-0.15 ± 0.02
500	-433 ± 81	-0.15 ± 0.04

[a] The reported uncertainties correspond to fitting errors. Since FSTO and SNTO frequency values do not conform to the theoretical model predictions, some systematic errors are present.

the minimum of the “wobble” curve, there is no direct way to map the matching position. Therefore adjusting tuning and matching reproducibly is rather difficult. In the end, we used the following rather simplistic approach on a probe with manual tuning and matching controls, which turned out to be effective and sufficiently reproducible. The amount of rotation was controlled by aligning marks at the bottom of the tuning and matching screws with a cross-hair mark drawn on a mirror placed below the probe. To map the signal response versus tuning and matching, the tuning screw was rotated in half turn increments and the matching adjusted in steps of quarter turns.

At each combination of tuning and matching positions thus adjusted, a spin noise spectrum was recorded using the block wise pseudo-2D method described previously.^[8] Before changing the tuning and matching settings the reference pulse spectra were acquired (the amplifier cables had to be de- and reconnected for each of these steps). The noise spectra were processed and the thermal noise level at each position was determined using short Matlab programs.

Determination of the FSTO

For Figure 2 experimental spectra were acquired on a Bruker Avance II 600 spectrometer equipped with a TXI cryo-probe built in 2008. The small flip angle spectra were acquired with a 0.33 μ s pulse at 3.8 W (corresponding to a 3° flip angle on resonance). The sample consisted of acetone 90% in [D₆]DMSO. The observed signal was the acetone one. The frequency shift curve in Figure 2d was obtained by plotting the chemical shift at the maximum of the NMR resonance signal exhibiting radiation damping against the tuning offset. The tuning offset was defined relative to the CTO. The C_i and C_m capacitances were optimized at a given offset to the lowest wobble curve by matching at 50 Ω . Note that in all experiments used for the study the reproducibility of the setting of the tuning position was limited by the mechanical properties of the probe assemblies to approximately ± 40 kHz. However, the offsets could be determined with a higher accuracy through the fitting procedures used. In addition to the small flip angle pulse experiments a pre-saturation pulse experiment was performed to attenuate radiation damping and obtain the reference shift. The latter can also be determined as the median of the spinning side bands, when spinning the sample slowly (ca. 10 Hz) or from the isosbestic intersection of the SFA spectra (Figure 2a). Apart from that, the frequency pushing is zero at the inflection point of the frequency pushing curve [Eq. (5)] and Figure 2d determined by curve fitting.

Using the frequency shifts and the line widths of the signals at each tuning position, it is possible to estimate the apparent quality factor *Q* of the probe without resorting to external hardware (for example, a network analyzer).^[10] Alternatively the entire curve was fitted to Equation (5) using the experimental (maximum) line width of the signal at zero frequency shift. The maximum observed line width of the signal from a sample containing 90% of acetone in [D₆]DMSO, was 124 Hz. The fitted apparent circuit quality factor *Q* was ~ 800 . It should be noted that the *Q*-values determined in this paper refer to the entire circuit as opposed to the coil only.

For Table 1 frequency shifts and tuning positions obtained on a 700 MHz TCI Bruker Avance III cryo-probe system (manufactured in 2011) were used to fit to Equation (5) to obtain the zero frequency shift and *Q*.

Conventional probe experiments were run on a Bruker Avance 500 spectrometer with a 5 mm BBI probe on an acetonitrile sample with 10 μ L of [D₆]DMSO used for field frequency locking. Series of small flip angle ¹H spectra were acquired for different cable lengths

and different tuning positions (varying CTO from 498.1 to 501.1 MHz). From tuning positions close to that leading to pure in-phase spin noise spectra, SNT0 conditions were determined by real-time monitoring of the electronic noise level while changing the tuning capacitor C_i.^[21] Spin noise spectra were acquired as a pseudo 2D map with very long acquisition times. The time domain data were split and Fourier transformed using a sliding window approach during the processing.^[4,21] Analogous procedures (frequency shift curves and comparison of the spin noise line shapes) were used for exploring effects of low temperatures or of changing the receiver gain levels.

Acknowledgements

Guillaume Ferrand and Michel Luong are warmly acknowledged for useful discussions on the detection circuit. Matlab scripts authored by Denis Marion were used in the processing of spin noise data. This research was supported by the Austrian Science Funds (FWF) and the Agence Nationale de Recherche (ANR) in the joint project IMAGINE (FWF project number I1115-N19, ANR project 12-IS04-0006) and by the EGIDE-ÖAD AMADEUS Austrian-French exchange program (no. 28948WD and FR 11/2013). The Avance III 700 MHz NMR spectrometer was co-financed by the European Union through the INTERREG IV ETC-AT-CZ program (EFRE RU2-EU-124/100-2010, project M00146 “RERI-uasb”).

Keywords: analytical methods • magnetic properties • NMR spectroscopy • radiation damping • spin noise

- [1] A. Abragam, *Principles of Nuclear Magnetism*, Clarendon, Oxford, 1961.
- [2] D. I. Hoult, R. E. Richards, *J. Magn. Reson.* **1976**, *24*, 71–85.
- [3] A. Vlassenbroeck, J. Jeener, P. Broekaert, *J. Chem. Phys.* **1995**, *103*, 5886–5897.
- [4] H. Desvaux, *Prog. NMR Spectrosc.* **2013**, *70*, 50–71.
- [5] M. Guéron, *Magn. Reson. Med.* **1991**, *19*, 31–41.
- [6] D. J.-Y. Marion, H. Desvaux, Patent, FRA 0708464, EP 2 068 164, **2007**.
- [7] D. J.-Y. Marion, H. Desvaux, *J. Magn. Reson.* **2008**, *193*, 153–157.
- [8] M. Nausner, J. Schlagnitweit, V. Smrčeki, X. Yang, A. Jerschow, N. Müller, *J. Magn. Reson.* **2009**, *198*, 73–79.
- [9] M. Guéron, J. L. Leroy, *J. Magn. Reson.* **1989**, *85*, 209–215.
- [10] D. A. Torchia, *J. Biomol. NMR* **2009**, *45*, 241–244.
- [11] J. Mispelster, M. Lupu, A. Briquet, *NMR Probeheads for Biophysical and Biomedical Experiments*, Imperial College Press, London, **2006**, p. 47.
- [12] M. Guenneugues, P. Berthault, H. Desvaux, *J. Magn. Reson.* **1999**, *136*, 118–126.
- [13] M. Nausner, M. Goger, E. Bendet-Taicher, J. Schlagnitweit, A. Jerschow, N. Müller, *J. Biomol. NMR* **2010**, *48*, 157–167.
- [14] N. Müller, A. Jerschow, *Proc. Natl. Acad. Sci. USA* **2006**, *103*, 6790–6792.
- [15] J. Schlagnitweit, J.-N. Dumez, M. Nausner, A. Jerschow, B. Elena-Herrmann, N. Müller, *J. Magn. Reson.* **2010**, *207*, 168–172.
- [16] J. Schlagnitweit, N. Müller, *J. Magn. Reson.* **2012**, *224*, 78–81.
- [17] J. Schlagnitweit, S. W. Morgan, M. Nausner, N. Müller, H. Desvaux, *ChemPhysChem* **2012**, *13*, 482–487.
- [18] E. Bendet-Taicher, N. Müller, A. Jerschow, *Conc. Magn. Res. B* **2014**, *44*, 1–11.
- [19] M. A. McCoy, R. R. Ernst, *Chem. Phys. Lett.* **1989**, *159*, 587–593.
- [20] K. Chandra, J. Schlagnitweit, C. Wohlschlagler, A. Jerschow, N. Müller, *J. Phys. Chem. Lett.* **2013**, *4*, 3853–3856.
- [21] H. Desvaux, D. J. Y. Marion, G. Huber, P. Berthault, *Angew. Chem.* **2009**, *121*, 4405–4407; *Angew. Chem. Int. Ed.* **2009**, *48*, 4341–4343.

Received: April 12, 2014

Published online on September 11, 2014